International Journal of Bioprinting

RESEARCH ARTICLE

3D printing of mechanically tough and self-healing hydrogels with carbon nanotube fillers

Soo A Kim[1], Yeontaek Lee[1], Kijun Park[1], Jae Park[1,2], Soohwan An[3], Jinseok Oh[1], Minkyong Kang[1], Yurim Lee[1], Yejin Jo[1], Seung-Woo Cho[3], Jungmok Seo[1,2]*

[1]School of Electrical and Electronic Engineering, Yonsei University, Seoul 03722, Republic of Korea

[2]LYNK Solutec Inc., Seoul 03722, Republic of Korea

[3]Department of Biotechnology, Yonsei University, Seoul 03722, Republic of Korea

(This article belongs to the *Special Issue: Convergence of 3D Bioprinting and Nanotechnology*)

Abstract

Hydrogels have the potential to play a crucial role in bioelectronics, as they share many properties with human tissues. However, to effectively bridge the gap between electronics and biological systems, hydrogels must possess multiple functionalities, including toughness, stretchability, self-healing ability, three-dimensional (3D) printability, and electrical conductivity. Fabricating such tough and self-healing materials has been reported, but it still remains a challenge to fulfill all of those features, and in particular, 3D printing of hydrogel is in the early stage of the research. In this paper, we present a 3D printable, tough, and self-healing multi-functional hydrogel in one platform made from a blend of poly(vinyl alcohol) (PVA), tannic acid (TA), and poly(acrylic acid) (PAA) hydrogel ink (PVA/TA/PAA hydrogel ink). Based on a reversible hydrogen-bond (H-bond)-based double network, the developed 3D printable hydrogel ink showed excellent printability via shear-thinning behavior, allowing high printing resolution (~100 μm) and successful fabrication of 3D-printed structure by layer-by-layer printing. Moreover, the PVA/TA/PAA hydrogel ink exhibited high toughness (tensile loading of up to ~45.6 kPa), stretchability (elongation of approximately 650%), tissue-like Young's modulus (~15 kPa), and self-healing ability within 5 min. Furthermore, carbon nanotube (CNT) fillers were successfully added to enhance the electrical conductivity of the hydrogel. We confirmed the practicality of the hydrogel inks for bioelectronics by demonstrating biocompatibility, tissue adhesiveness, and strain sensing ability through PVA/TA/PAA/CNT hydrogel ink.

Keywords: Hydrogels; 3D Printing; Toughness; Self-healing; Nanofillers; Bioelectronics

***Corresponding author:**
Jungmok Seo
(jungmok.seo@yonsei.ac.kr)

Citation: Kim SA, Lee Y, Park K, *et al*., 2023, 3D printing of mechanically tough and self-healing hydrogels with carbon nanotube fillers. *Int J Bioprint,* 9(5): 765. https://doi.org/10.18063/ijb.765

Received: February 6, 2023
Accepted: April 18, 2023
Published Online: May 31, 2023

1. Introduction

Bioelectronics are functional devices that integrate biomolecules and electronic elements to measure biosignals from various parts of the human body, including the skin, heart, spinal cord, and brain[1,2]. Thus, they are at the core of emerging applications in the medical field such as healthcare monitoring devices, drug delivery systems, and implantable devices[3-5]. Despite the significance of bioelectronics in advanced healthcare

systems, there remain some inherent dissimilarities between rigid electronic devices and soft biological tissues, presenting a challenge to the seamless operation of human–machine interfaces[6,7]. Therefore, there has been increasing interest in the development of soft, flexible, and stretchable electronics and robotics made from soft materials to address these issues in bioelectronics.

Hydrogels, which are three-dimensional (3D) crosslinked polymer networks containing large amounts of water, have gained considerable attention for their potential in bioelectronics[8,9]. The soft and flexible nature of hydrogels reduces the mechanical mismatch with human tissues, making them an attractive option for bridging the gap between electronics and human tissues due to their biocompatibility and flexibility in controlling their electrical, mechanical, and biological properties[10]. However, there are still some challenges to overcome for their widespread use in bioelectronics. The mechanical weakness and brittleness of these water-soluble polymers under large deformation and physical stress make them unsuitable for most load-bearing physiological situations and bioelectronics applications[11].

Furthermore, the lack of self-healing properties, which is a characteristic of human tissues, can lead to irreversible collapse during bioelectronic operations[12]. To address these problems, self-healing hydrogels with reversible networks via breakage and reformation of bonds have been widely studied in recent years. Self-healing hydrogels that can automatically repair themselves from external damages have the potential to restore their original features[13], thus integrating the self-healing ability into electrical devices can extend the lifetime of the device[14,15].

In addition, for the successful application of hydrogel-based bioelectronics, a fabrication method that can produce individualized shapes and complex structures is crucial[16]. 3D printing presents a promising solution to this requirement as it offers the ability to produce hydrogels with high precision and geometric freedom[17]. However, transforming bulk hydrogels into intricate designs and patterns with high resolution (~100 μm) is still a challenge and remains in its early stages of research, hindering the practical use of hydrogels[7,12]. To date, several attempts have been made to fabricate multi-functional hydrogels that possess 3D-printing capabilities, toughness, and self-healing to improve their durability and practicability for their practical use. However, it still continues to pose a difficulty to fulfill all of those features, and in particular, many researchers reported self-healing and tough hydrogel electronics but have not been incorporated with 3D printability and high resolution of printing fidelity[18]. For example, Chen *et al.*[19] represented stretchable, self-healing, and printable hydrogels, fabricated by triggering the *in situ* polymerization of a polyaniline/poly(4-styrenesulfonate) (PANI/PSS) network which exhibits the dynamic and reversible nature of the non-covalent crosslink. Similarly, Jin *et al.*[20] reported on conductive and adhesive cellulose (CAC) hydrogel ink with self-healable and printable features mixed with tannic acid (TA) and various metal ions. Although these multi-functional hydrogels provide self-healing, conductive, and printable properties, they still possess poor printing fidelity with low resolution (over 0.6 mm) and have not been extended to printing in 3D structures. Meanwhile, Wei *et al.*[21] reported a super tough and printable agar/polyacrylamide (PAAm)-based double network hydrogel. The agar/PAAm hydrogel, owing to the alginate acting as a crosslinker, exhibited suitable viscosity as a printable ink with good mechanical properties. Despite the improved mechanical properties[21], low 3D-printing resolution and the lack of self-healing capability limit their practical use as 3D printable hydrogel inks.

To achieve seamless human–machine interfaces in hydrogel-based bioelectronics, the development of multi-functional hydrogels with all of the desired features, including 3D printability with high resolution, toughness, and self-healing ability, is urgently needed.

Herein, we present a novel multi-functional hydrogel ink that is 3D printable, tough, self-healing, and conductive. The ink is composed of poly(vinyl alcohol) (PVA), tannic acid (TA), and poly(acrylic acid) solution (PAA). PVA is used as the base material due to its biocompatibility and tissue-like softness, which is achieved through hydrogen bonding (H-bond). However, pure PVA is mechanically weak and not printable. Thus, TA is added as a crosslinker to form weak and reversible H-bonds in the PVA hydrogel, and PAA is introduced to form a double network by forming strong H-bonds. This strong and weak crosslinking H-bond-based double network-enabled PVA/TA/PAA hydrogel ink exhibits 3D printability, mechanical toughness, and self-healing properties. Since TA provided sufficient crosslinking sites for the formation of reversible H-bonds, breakage and reformation of H-bonds could occur spontaneously even at high temperatures (over 80°C). This enabled the proposed hydrogel inks to be 3D printable, as they exhibited suitable viscosity for printing under heat and maintained a robust printed structure. The rheological behavior and tensile tests were evaluated to optimize the printable and mechanical properties of the PVA/TA/PAA hydrogel ink, and it was found that the optimized ink had shear-thinning behavior, leading to excellent 3D-printing fidelity with high resolution (~100 μm). The hydrogel ink displayed good toughness, with a tensile strength of ~45.6 kPa, an elongation at break of ~650%, and Young's modulus of

~15 kPa. It also had self-healing properties, being able to recover from a break within 5 min. Carbon nanotubes (CNTs) were incorporated into the PVA/TA/PAA hydrogel ink as nanofillers to improve its electrical conductivity, and the applicability of the PVA/TA/PAA/CNT hydrogel ink was confirmed through *in vitro* biocompatibility and tissue adhesiveness with the chemical functionalization of the hydrogel chain. Also, light-emitting diode (LED) lighting tests and resistance change via a printed circuit with PVA/TA/PAA/CNT hydrogel ink showed the possibility of a strain sensor.

2. Materials and methods

2.1. Preparation of PVA/TA/PAA hydrogel ink

To prepare hydrogel ink, the 4000 mg of PVA (Sigma-Aldrich, St. Louis, MO, USA, 20% w/w, Mw 89,000–98,000) powder was added to deionized (DI) water, heated at 90°C, and continuously stirred to obtain a transparent solution. After 20 min, TA (Sigma-Aldrich, St. Louis, MO, USA) at different ratios (PVA: TA = 1:0.5, 1:1, and 1:2) was added to the PVA solution and stirred for 2 h to obtain a homogeneous PVA/TA solution. The PVA/TA solution was then poured into a mold, pressed to be spread thinly and widely, stored in a refrigerator at -20°C for 8 h, and thawed at 25°C for 4 h to form a PVA/TA hydrogel. The PVA/TA hydrogel was dried in an oven at 37°C for 1 h and annealed at 100°C for 1 h to obtain a dry PVA/TA film. To form the PVA/TA/PAA network, PVA/TA film was immersed in 45 mL of aqueous acrylic acid solution (30% w/w acrylic acid, 0.03% w/w N, N′-bis(acryloyl)cystamine, and 0.15% w/w 2,2′-azobis(2-methylpropionamidine) dihydrochloride in deionized water) for 2 h. The soaked hydrogel was heated at 70°C for 30 min to form the PAA network. To prepare the pure PVA hydrogel and PVA/PAA hydrogel, we used a PVA hydrogel without TA but otherwise followed the same process.

2.2. Preparation of PVA/TA/PAA/CNT hydrogel ink

The COOH functionalized CNT powder (Nano-lab, USA, outer diameter of 30 ± 15 nm, length of 1–5 μm) was dispersed in 10 mL of DI water to concentrations of 1, 3, 6, and 9 mg/mL. Each solution was sonicated at 450 rpm for 2 h using a tip sonicator (Qsonica LLC, Newtown, CT, USA) to obtain a homogenous CNT solution. The CNT solution was added to the PVA/TA hydrogel and stirred for an additional 2 h while heating at 90°C. The resulting CNT/PVA/TA hydrogel underwent freezing at -20°C and thawing at 25°C, and the same process was used to form the PAA network.

2.3. Rheological characterization of hydrogel ink

The rheological properties of the hydrogel inks were characterized using an MCR 102 Anton Paar rheometer (Anton Paar GmbH, Austria), with a parallel plate geometry, equipped with a 25-mm plate with a distance of ~1 mm. The shear storage modulus (G′) and loss modulus (G″) were measured with temperature scans ranging from 25°C to 95°C at a constant shear strain of 1% and frequency of 10 radian/s. The shear viscosity of the hydrogel was measured in steady-state flow at a logarithmic sweep of shear rates from 0.1 s^{-1} to 100 s^{-1} to investigate the shear-thinning behavior at 85°C.

2.4. 3D printing of hydrogel ink

All printing was performed using an EZROBO-5GX 3D printer with an AD3300C dispenser (Iwashita, Japan), equipped with a nozzle and temperature controller. During printing, ink was heated to 85°C using a temperature control system and syringe heating pad, and various nozzle sizes (600-, 400-, 200-, and 100-μm size of nozzles) were used. Printing structures were designed using Ez-EDITOR robot communication software. The diameters of the printed hydrogels were compared with those of the printing nozzle using a field-emission scanning electron microscope (FE-SEM, JSM-IT-500HR, JEOL, Japan) at an accelerating voltage of 15.0 kV with gold sputtering to enhance image contrasts.

2.5. Mechanical characterization of hydrogel ink

The mechanical properties of the hydrogels were characterized using a tensile testing machine (MultiTest 2.5-DV, Mecmesin, UK) with a 50 N load cell at a speed of 50 mm/min to determine their ultimate tensile strength and elongation at break. The bulk hydrogel ink samples were cut to a size of 200 mm (height) × 100 mm (width). The printed hydrogel ink samples of 200 mm (height) × 100 mm (width) were manufactured using the above-mentioned EZROBO-5GX 3D printer with a nozzle size of 600 μm. For the tensile tests, at least three samples of each type were tested and averaged to determine their properties.

2.6. Swelling ratio measurement

The hydrogels were soaked in DI water at room temperature to determine their swelling ratio. All hydrogel samples were prepared with similar weights and the same pattern. After swelling for the desired time, the swollen hydrogels were removed from water and weighed. The weights of the samples were recorded at 0, 30, 60, 120, 240, 480, and 960 min after removal, and the swelling ratio was calculated using the following Equation I:

$$\text{Swelling ratio}(\%) = \frac{W_t - W_i}{W_t} \times 100(\%) \quad \text{(I)}$$

where W_i and W_t are the weights of the initial and swollen hydrogel, respectively.

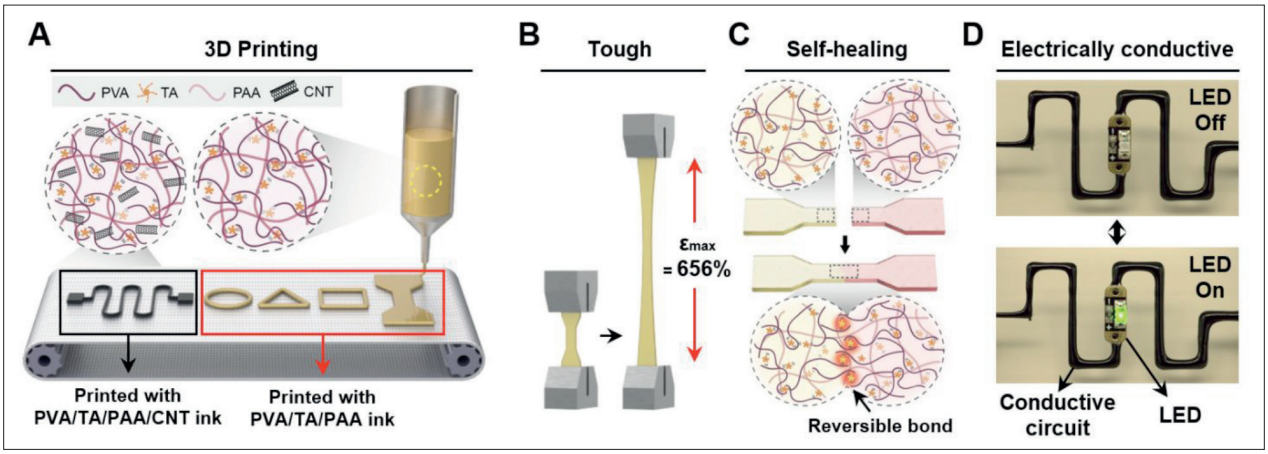

Figure 1. The overall characteristics of developed multi-functional hydrogel ink. (A) Schematic illustration of 3D-printable hydrogel ink material components and the printed architecture. (B, C) Illustration of mechanically tough and self-healing properties of PVA/TA/PAA hydrogel ink. (D) Electrically conductive performance of PVA/TA/PAA/CNT hydrogel inks through LED lighting tests.

2.7. Tissue adhesion and *in vitro* biocompatibility tests

To enable the hydrogel adhesive property, N-hydroxysuccinimide ester (NHS) ester groups were introduced into the hydrogel. The PVA/TA/PAA/CNT hydrogel was soaked in a 2-(N-morpholino) ethanesulfonic acid (MES) buffer containing 1-ethyl-3-(-3-dimethylaminopropyl) carboiimide (0.5% w/w) and NHS sodium salt (0.25% w/w) for 5 min at room temperature. Adhesion tests were conducted with porcine skin substrates, and the hydrogel was placed on the porcine skin substrates.

For the *in vitro* biocompatibility test, the PVA/TA/PAA and PVA/TA/PAA/CNT hydrogel samples were prepared with a size of 10 mm (height) × 10 mm (width) × 1 mm (thickness). Then, the NIH-3T3 fibroblast cells (0.5×10^5 cells per mL) were directly cultured with the prepared hydrogel in 1 mL of DMEM supplemented with 10% bovine calf serum and 1% penicillin–streptomycin. A viability test was carried out using a Live/Dead kit (L3224, Invitrogen, USA) according to the manufacturer's instructions. To visualize the viability of the cells, a laser scanning confocal microscope (LSM700, Carl Zeiss, Germany) with a 10× magnification was used.

2.8. Electrical conductivity measurement and LED test

The electrical conductivity of the PVA/TA/PAA/CNT hydrogel ink was measured using a modified four-point probe method with an AC voltage (±1 V, 1000 Hz). The conductivity was recorded using a probe station (MST4000A, MSTECH, Korea). As with the tensile samples, conductivity measurement samples were prepared with dimensions of 20 mm (length) × 10 mm (width). The bulk PVA/TA/PAA/CNT hydrogel inks were cut into rectangular shapes, accordingly. Electrical conductivity (σ) was calculated using the following Equation II:

$$\sigma = \frac{L \times I}{W \times T \times V} \quad \text{(II)}$$

where I, V, L, W, and T are the current flowing through the sample and the voltage, length, width, and thickness of the sample, respectively.

The length, width, and thickness were measured using an optical microscope (SMZ645; Nikon, Japan). To further demonstrate the conductive features of the PVA/TA/PAA/CNT hydrogel ink, an electronic circuit was designed to switch on an LED (Adafruit, USA) with a printed hydrogel as a conductor and a 30 V DC supply (RIGOL Technologies DP832, Beijing, China).

3. Results and discussion

3.1. Multi-functional 3D-printed hydrogel ink

For reliable, long-term, and practical hydrogel-based bioelectronics, not only must the hydrogels exhibit tough and stretchable properties, but self-healing 3D printable fabrication, and conductivity must also be realized. Previously studied hydrogels mostly lack one or more of these combined functions. Therefore, we aimed to develop a multi-functional hydrogel that is 3D printable, tough, self-healing, and electrically conductive on one platform (Figure 1). As shown in Figure 1A, a 3D printable hydrogel ink was successfully synthesized by mixing PVA, TA, and PAA. In addition, CNT was added to the PVA/TA/PAA ink to fabricate conductive PVA/TA/PAA/CNT inks, and the hydrogel inks were successfully printed into various shapes with high resolution. The resulting PVA/TA/PAA

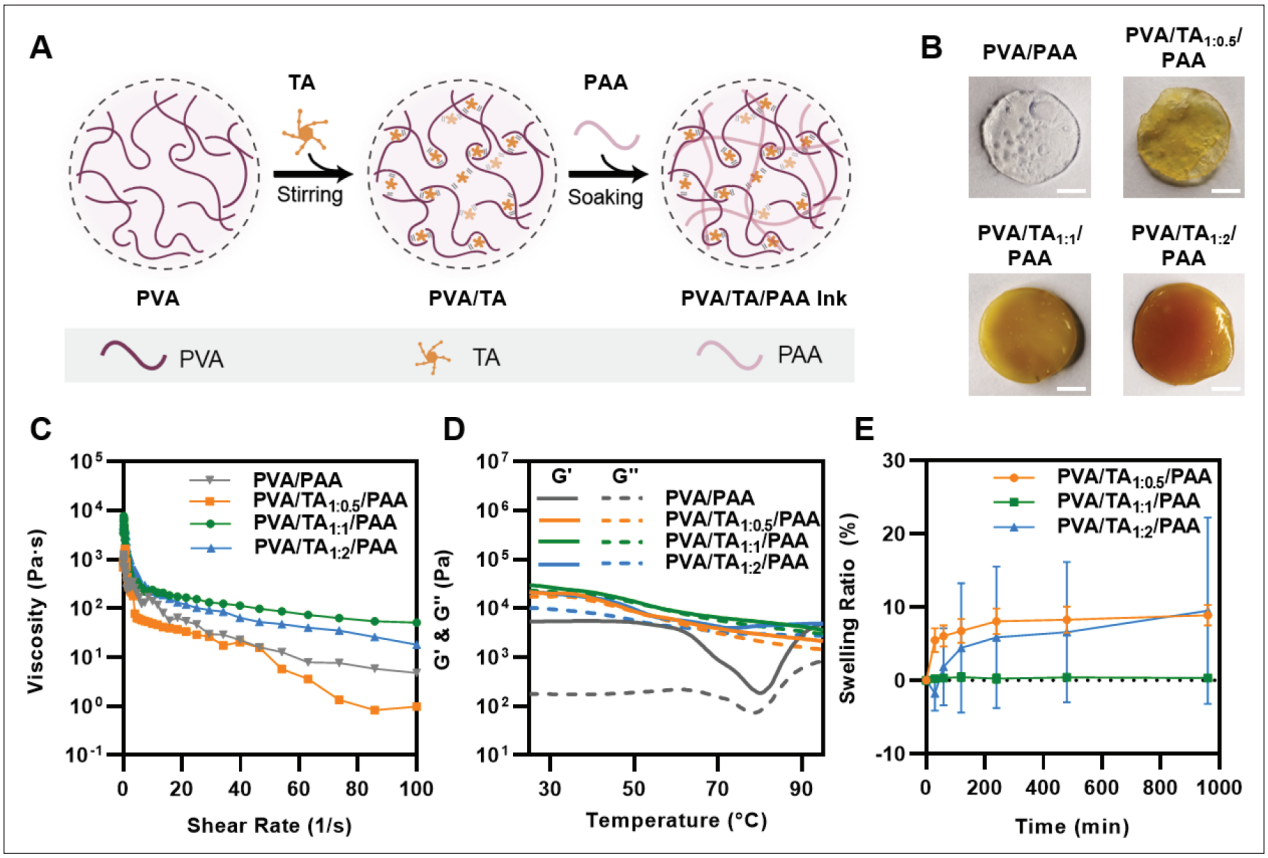

Figure 2. Material preparations and rheological measurements of hydrogel inks. (A) Schematic illustration of the synthesis process of PVA/TA/PAA hydrogel inks. (B) The sample preparation of different mass ratios of PVA and TA (no TA, 1:0.5, 1:1, and 1:2). The scale bar is 5 mm. (C) Viscosity as a function of shear rate. (D) Storage modulus (G′) and loss modulus (G″) as a function of temperature. (E) Swelling ratio of printed PVA/TA/PAA hydrogel inks in DI water.

hydrogel ink exhibited excellent mechanical properties due to its reversible H-bond-based double network. The combination of strong and weak H-bonds in the double network gave the hydrogel ink tough and self-healing properties, as depicted in Figure 1B and C.

Additionally, the CNT filler incorporated into the PVA/TA/PAA hydrogel inks enabled electrical conductivity. To demonstrate this conductive property, a simple LED lighting circuit was printed using the conductive PVA/TA/PAA/CNT hydrogel ink (Figure 1D), highlighting the potential of hydrogel inks as soft materials for bioelectronics.

3.2. Synthesis process of PVA/TA/PAA hydrogel ink

Figure 2A shows a schematic illustration of the PVA/TA/PAA hydrogel ink synthesis process. PVA was chosen as the base material owing to its excellent biocompatibility, flexibility, and tissue-like softness[22]. The abundant hydroxyl groups on its backbone enable excellent water retention, thereby improving processability[23]. However, as aforementioned, pure PVA hydrogel ink exhibits poor 3D-printing performance, in that extrusion is not continuous and uniform. Moreover, in terms of mechanical properties, PVA hydrogels are weak which makes them unsuitable as material for bioelectronics[24]. Thus, TA was added as an effective binder to crosslink with the PVA chain to form intermolecular H-bonds[25]. TA is a natural water-soluble polyphenol compound rich in pyrogallol and catechol groups[26]. Due to the large number of hydroxyl groups present in a TA molecule, a weak and reversible H-bond is formed between PVA and TA[27]. The weak and reversible H-bonds of TA can effectively break and spontaneously reform; thus, the crosslinked intermolecular structures enabled the reformation of H-bonds after physical damage, resulting in a self-healing capability even after subjection to heat from printing[28,29]. Thereafter, the homogeneously stirred PVA/TA hydrogels were soaked in an aqueous PAA solution to form double network hydrogel inks. The carboxyl groups on the PAA chains are capable of forming strong H-bonds; hence, strong intermolecular interactions were formed in the PAA chains[30]. In addition, N, N′-bis(acryloyl)

cystamine in PAA solution also imparted self-healing properties. N, N′-bis(acryloyl)cystamine acted as a crosslinking agent with a disulfide bond[31,32]. Disulfide bonds, along with hydrogel bonds, contributed to self-healing properties as a type of reversible bond. Through the double network of the strong H-bonds with disulfide bond within the PAA chain and the weak H-bonds of PVA/TA, desirable properties were obtained: the H-bond-based double network endowed toughness via energy dissipation mechanism that enabled maintaining strong H-bonds from physical damage by dissipating energy as weak H-bonds are broken, and the rapid breakage and reformation of weak H-bonds imparted stretchability and self-healing ability[33].

In particular, the addition of TA was most influential in enabling the printing of the proposed hydrogel ink. Even if a high temperature (over 80°C) is applied to the hydrogel ink for extruding from a precise nozzle and, consequently, a weak bond is broken, reformation of the H-bond rapidly occurs again immediately after deposition, enabling the ink to maintain its robust printed structure. To investigate the optimal composition of high-performance hydrogel inks, inks were prepared with different mass ratios of PVA and TA. As shown in Figure 2B, PVA/TA/PAA hydrogels with varying PVA and TA mass ratios (no TA, 1:0.5, 1:1, and 1:2) were successfully formulated, and their material characteristics were investigated.

3.3. Rheological properties and swelling behavior test

To ensure the functionality of bioelectronics through the manufacturing of hydrogels into specific shapes and patterns, the hydrogel inks used for printing must meet certain requirements, including shear-thinning properties and shape fidelity[34,35]. To evaluate the suitability of the hydrogel ink for printing, the viscosity of hydrogel was tested at different mass ratios under varying shear rates (Figure 2C). Under heat treatment at 85°C, all tested hydrogel inks exhibited shear-thinning behavior with high viscosity at a low shear rate (10^{-1} s^{-1}) and low viscosity at a high shear rate (10^{2} s^{-1}), as a result of weak H-bond breakage. To further assess the thermal response of the hydrogel inks, the changes in the storage modulus (G′) and loss modulus (G″) were measured with temperature changes from 25°C to 95°C (Figure 2D). Notably, the results showed that the G′ of the PVA/PAA hydrogel without TA was larger than G″ within the tested temperature range, with G′ dominating even at high temperature. This indicates that the PVA/PAA hydrogel is in a gel state with elastic behavior regardless of the temperature (within the tested range), which is inappropriate for printing to extrude from the narrow and fine nozzle. In addition, it showed that G′ and G″ are quickly dropped at about 80°C. Due to the absence of TA, PVA/PAA ink, which could not form a reversible double bond, caused breakage of crosslinking sites in it by heat, resulting in a sharp decrease in modulus. However, the PVA/TA/PAA hydrogel exhibited overall similar results, with both G′ and G″ decreasing continuously with increasing temperature. The gap between G′ and G″ was small and sometimes reached equal values, indicating that the inks were in the sol-gel state, which is suitable for printing to effectively flow from the precise nozzle. These observations (Figure 2C and D) suggest that PVA/$TA_{1:1}$/PAA hydrogel ink is the most printable of all ink compositions. Because the ratio between PVA and TA affected the formation of a reversible double network and crosslinking density in the PVA/TA/PAA hydrogel ink, too low or too high concentration of TA led to a decrease of the viscosity and moduli. PVA/$TA_{1:1}$/PAA hydrogel ink displayed the highest viscosity reaching approximately 100 Pa·s at 100 s^{-1}, and the highest moduli, with both G′ and G″ reaching about 10 kPa at 85°C, which indicates that the ratio of 1:1 is most suitable for the rheological property. In addition, curves of the temperature and the angular frequency-dependent G′ and G″ of PVA/$TA_{1:1}$/PAA hydrogel ink showed that G′ was higher than G″ in all the temperature and frequency regions. This suggests that the weak H-bonds can reform from external stimuli, preserving the double network and allowing the inks to maintain their structure after printing layer by layer without collapsing (Figure 2D; **Figure S1** in Supplementary File).

The swelling tests also showed that the 1:1 ratio of PVA and TA is optimal for the formation of a crosslinked network. The different ratios of PVA and TA were printed in the same structure, immersed in DI water for 960 min, and weighed at various time points. As shown in Figure 2E, PVA/$TA_{1:1}$/PAA hydrogel showed almost 0% of swelling ratio with no increase in its weight. However, PVA/$TA_{1:0.5}$/PAA quickly expanded to a swelling ratio of 7.5% within 240 min, since too low concentration of TA does not offer sufficient crosslinking sites to form H-bond. Meanwhile, the weight of the PVA/$TA_{1:2}$/PAA hydrogel decreased to a swelling ratio of -3.7% within the first 100 min and rapidly expanded up. This is because the concentration of TA was too high to mix homogeneously in the hydrogel network, which led the network inside PVA/$TA_{1:2}$/PAA hydrogel to prevent the formation of dense crosslinking. As a result, when the high temperature was applied to the hydrogel and the weak bonds are broken, the reformation of the H-bond and disulfide bond by the self-healing mechanism does not rapidly occur. Thus, by the breakage of the hydrogel network after printing, the aggregated TA is released and washed out with DI water. We also calculated the water content of hydrogel by dividing the weight of the

dried hydrogels by the wet hydrogels; dried hydrogels were all prepared being frozen and dried in a vacuum freeze dryer. The water content of the printed PVA/TA/PAA hydrogels with the mass ratio of 1:0.5, 1:1, and 1:2 was about 70.8%, 92.4%, and 83.5%, respectively (**Figure S2** in Supplementary File). The results showed less increment of swelling ratio in higher water content, and these can be attributed to the crosslinking density and the internal hydrogel network. In particular, PVA/$TA_{1:1}$/PAA hydrogel showed high water content and non-swellable property after immersing DI water. It indicates that hydrogel can operate stably even in a wet environment in the application of bioelectronics.

3.4. Printability and 2D-, 3D-printing performance

We utilized the rheological properties of the hydrogel ink to print a certain architecture for evaluated PVA/TA mass ratios. Figure 3A presents the results of printing fidelity for the various hydrogel ink compositions. All inks were printed using the same design with a 600-μm diameter nozzle, and the PVA/$TA_{1:1}$/PAA hydrogel ink produced uniform and precise results. The filament extruded from the nozzle was uniform, achieving a width similar to that of the nozzle, and the designed structure was precisely printed with a sharp edge. Its high viscosity and moduli allowed it to maintain its structure after being extruded from the nozzle. In contrast, the PVA/$TA_{1:0.5}$/PAA and PVA/$TA_{1:2}$/PAA hydrogel inks had low printing accuracy, with the filaments not retaining their shape and the printed structures losing their details and sharpness. As explained above, TA did not form dense crosslinks owing to the low concentration of TA and not homogeneously mixed in ink due to too high a concentration of TA. Consequently, when the ink was heated for extrusion from the nozzle and the weak H-bonds were broken, the bonds were unable to rapidly reform the H-bond to maintain a robust printed structure. The high-resolution printing capability of the PVA/$TA_{1:1}$/PAA hydrogel was demonstrated by printing 2D shapes through 400-, 200-, and 100-μm diameter nozzles (Figure 3B) and mesh structures using a 100-μm diameter nozzle (Figure 3C). The SEM images confirmed the high pattern fidelity of the printed scaffolds, with a continuous filament and precise grid. Additionally, the favorable rheological properties of the PVA/$TA_{1:1}$/PAA hydrogel ink allowed us to fabricate multi-layered 3D structures through layer-by-layer stacking with a 600-μm nozzle, which was strong enough to support their own weight (Figure 3D). In particular, all printing procedures were conducted without any post-processing but showed high resolution and 3D printability. Recently, Zhou *et al.*[36] presented 3D printing of a UV-curable elastomer with digital light processing. 3D printing with digital light processing is a rapidly developing area since it enables the hydrogel with high resolution and fine printing structure. The literature showed a high resolution (~60 μm) of the resultant printed structure with high stretchability (stretched up to over 800%). However, it required about 10–20 min after printing for the curing and cleaning time, which is the typical disadvantage of digital light processing printing that leads the process complicated and hampers the practicality. Compared to this printing process, the proposed PVA/TA/PAA hydrogel ink can be efficiently printed in 3D and retain its structure without post-process while maintaining mechanical properties including toughness, stretchability, and self-healing ability. Furthermore, regarding the resolution of hydrogel, PVA/TA/PAA hydrogel has a high printing performance compared to other studied printable multi-functional hydrogels[37].

3.5. Mechanical and self-healing properties of PVA/TA/PAA hydrogel ink

To minimize the mismatch between human tissue and electronic devices, it is important for the mechanical properties of the hydrogels used to be similar to those of human tissue while still being strong enough for long-term bioelectronics functionality[38]. The mechanical properties of the hydrogel inks with different PVA to TA ratios (1:0.5, 1:1, and 1:2) were evaluated through tensile tests. Figure 3E shows the typical stress–strain curve for each ratio of the printed hydrogel. It is apparent that there is a trade-off between toughness and stretchability; as the TA ratio increases, elongation increases but maximum tensile strength decreases (**Figure S2** in Supplementary File). For low TA ratios (PVA/$TA_{1:0.5}$/PAA), crosslinking sites cannot be sufficiently formed in the hydrogel network, resulting in poor stretchability. In addition, for high TA ratios (PVA/$TA_{1:2}$/PAA), the hydrogel network does not homogeneously mix with TA, causing it to aggregate and reduce toughness (**Figure S3** in Supplementary File). The PVA/$TA_{1:1}$/PAA hydrogel ink was found to have the most balanced mechanical properties, offering both high toughness and stretchability. Its maximum tensile strength and elongation at break were 45.6 kPa and 656%, respectively. Then, the mechanical properties of the printed PVA/$TA_{1:1}$/PAA hydrogel ink were compared to those of the bulk hydrogel (Figure 3F). As shown in Figure 3G, the maximum tensile strength of the bulk and printed hydrogel is not significantly differed and showed both high toughness with stretchability. Despite the heat applied to the hydrogel for printing, the printed hydrogel showed high toughness and elongation at break up to 600%. However, Young's modulus of printed hydrogel was decreased compared to the bulk hydrogel. This is attributed to the dehydration of hydrogel after printing (**Figure S4** in Supplementary File). When a hydrogel is dehydrated, as its volume decreases, the hydrogel shrinks and the network of the hydrogel

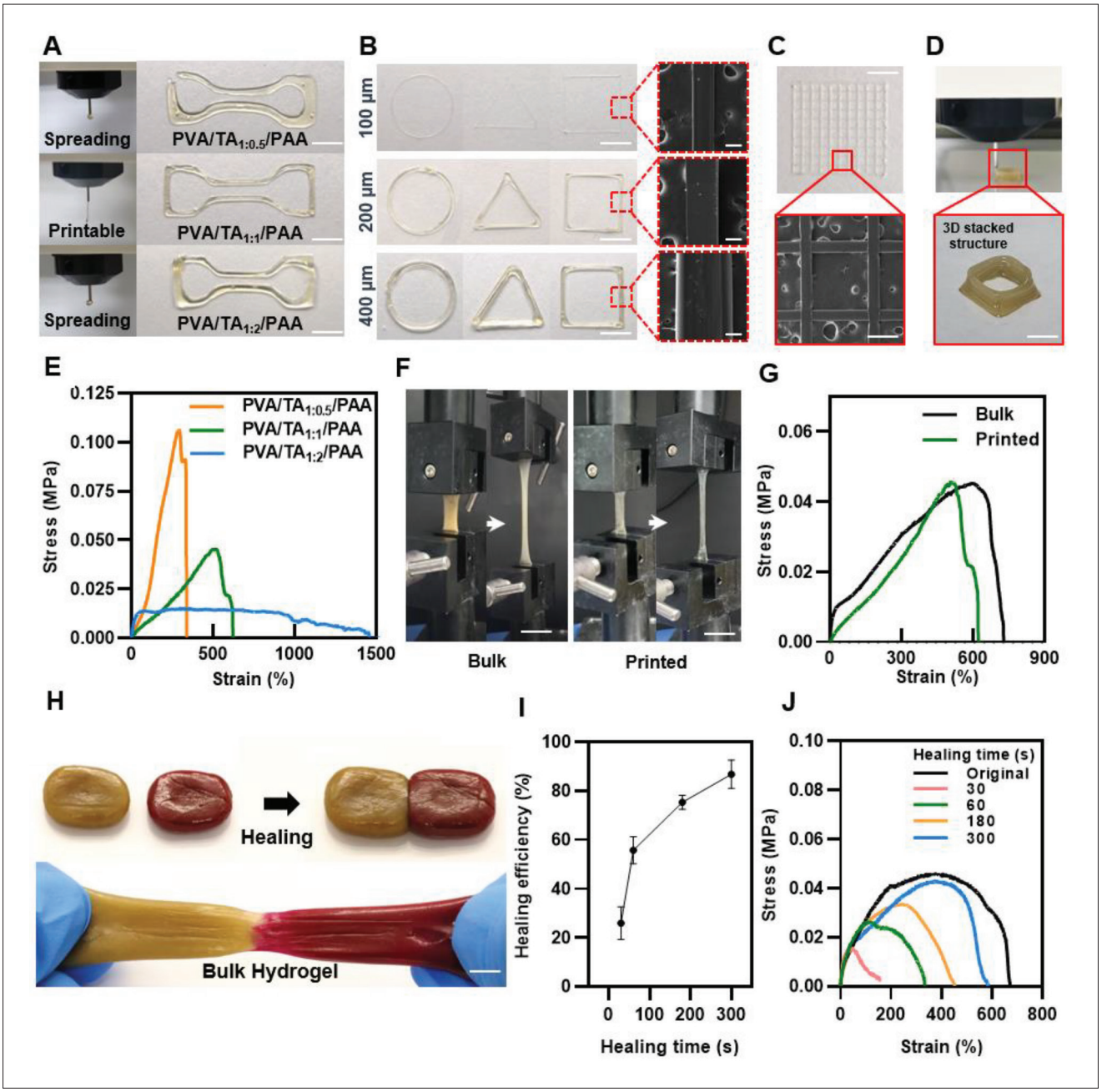

Figure 3. Printability and mechanical properties of hydrogel inks. (A) Photographic images of printing filament and printed structure with different mass ratios of PVA and TA. (B) 2D-printing performance of various shapes with PVA/$TA_{1:1}$/PAA hydrogel inks through 400-, 200-, and 100-μm diameter nozzles, and SEM images. (C) Printed meshes structures of 2D printing and SEM image. (D) 3D-printed hydrogel by stacked structure. (E) Stress–strain curves of each ratio of printed hydrogel inks. (F) Optical image of the bulk and printed PVA/$TA_{1:1}$/PAA hydrogel mechanical properties. (G) Stress–strain curves of the bulk and printed PVA/$TA_{1:1}$/PAA hydrogel ink. (H) Photographs of the self-healing hydrogel. (I) Self-healing efficiency of the hydrogel as a function of healing time ($n = 3$: n is the sample size). (J) Stress–strain curves of self-healed hydrogel for each time point. (Scale bar: 5 mm for (B), 100 μm for SEM image of (B), 500 μm for (C), 5 mm for (D), 10 mm for (F), and 7 mm for (H)).

is pulled closer, which can lead to a decrease in Young's modulus. But it still showed tissue like Young's modulus (~15 kPa), which falls within the range exhibited by soft tissue (10–100 kPa) and is suitable for implementation in bioelectronics[7].

Further, the evidence of the self-healing ability of both the bulk PVA/$TA_{1:1}$/PAA hydrogels is displayed in Figure 3H. For better visualization, a self-healing test was conducted using PVA/$TA_{1:1}$/PAA hydrogel dyed with rhodamine B, and the two separated hydrogel samples were placed

together. The samples were brought into contact, and after 3 min, they had self-healed to form an integrated structure and could withstand stretching, and also the printed PVA/$TA_{1:1}$/PAA hydrogels displayed self-healing ability within 3 min (**Figure S5** in Supplementary File). Then, by comparing the original maximum (N) tensile strength and the tensile strength after self-healing (N'), the self-healing efficiency of the bulk hydrogel, (N'/N) ×100 (%), was calculated at various time points (Figure 3I). It revealed a 30% recovery in 30 s, and the healing efficiency increased dramatically as the time increased, showing self-healed 80% after 5 min. Figure 3J is the results of strain–stress curve tested with the hydrogels after self-healing times at 30, 60, 180, and 300 s. As previously explained, this rapid autonomous self-healing ability is a result of the weak H-bond formation of TA in the PVA/TA/PAA network and the disulfide bond within PAA, which enables the breakage and reformation of reversible bonds[29]. Afterward, the maximum tensile tests after self-healing in 180 s with different value of pH and temperature were also investigated (**Figure S6** in Supplementary File). The pH did not significantly affect the self-healing property, which is due to the non-swellable characteristics of PVA/$TA_{1:1}$/PAA hydrogel, as confirmed in the previous swelling ratio test. Meanwhile, when the strain–stress curve tests of the hydrogel according to temperature were conducted, it showed that the higher the temperature applied, the lower the tensile strength of the hydrogel, but the better the stretchability. It elongated to 890% when heated to 85°C. As shown in Figure 2D of the rheological property, when the temperature is applied, the storage and loss modulus of the hydrogel decreases. Hydrogels with a lower storage and loss modulus tend to be more stretchable, as they can dissipate less energy and withstand larger deformation.

3.6. Synthesis process and characterization of PVA/TA/PAA/CNT hydrogel ink

Electrically conductive hydrogels using various types of conductive materials such as carbon nanotube-based and graphene-based materials have been developed for bioelectronics[39]. However, one of the main challenges of the incorporating such nanoparticles or nanotubule-doped hydrogels is achieving a homogeneous dispersion of the particles within the hydrogel matrix[40]. Aggregation of the particles hinders the dense crosslinking within the hydrogel matrix, which leads to poor mechanical properties and rheological properties, thus preventing the tough, self-healing, and printable hydrogel implementation. In addition, some nanoparticles, such as certain types of metal nanoparticles, have been shown to have toxic effects on tissues[41], therefore not suitable for biomedical applications. To address these problems, we attempted to realize a tough, self-healing, and printable conductive hydrogel ink using our proposed hydrogel in combination with additional CNT fillers. Compared to previously reported hydrogel with multi-functionality (**Table S1** in Supplementary File), the proposed hydrogel, which implemented the features of conductivity, toughness, stretchability, self-healing ability, and 3D printability in one platform showed excellent performance especially in self-healing with rapid recovery and printability with high resolution.

CNT functionalized with a carboxyl group was used since it is water soluble and can be distributed within our PVA, TA, and PAA-based hydrogel network via H-bond through their carboxyl and hydroxyl groups[42]. As shown in Figure 4A, the carboxyl functionalized CNT with DI water was sonicated and poured into the PVA/TA hydrogel at a mass ratio of 1:1. PAA was then introduced into the PVA/TA/CNT hydrogel to obtain the PVA/TA/PAA/CNT ink. To prove whether the CNT was mixed into the PVA/TA/PAA hydrogel without significant impairment of existing features, the rheological properties of an ink with CNT concentration of 6 mg/mL were investigated in terms of its printability and mechanical properties. It exhibited a shear-thinning effect in which viscosity decreased as the shear rate increased and both G' and G" decreased monotonously as temperature increased, with similar values of G' and G" (**Figure S7** in Supplementary File). Based on these rheological measurements, the printability of PVA/$TA_{1:1}$/PAA/CNT hydrogel inks was verified by examining printing fidelity using nozzles of various diameters and successfully printed a 3D structure through layer-by-layer stacking (**Figure S8** in Supplementary File). The mechanical properties of bulk PVA/$TA_{1:1}$/PAA/CNT hydrogels with CNT concentrations of 0 (without CNT), 1, 3, 6, and 9 mg/mL were also verified as shown in Figure 4B. The measured stress–strain curves represented that as CNT incorporation increased, the maximum tensile strength improved while the elongation at break was reduced. Although the stretchability of the hydrogel was weakened compared to without CNT hydrogel, the results showed a consistent tendency that the tensile strength was enhanced according to the CNT concentration. It indicates that the CNTs were homogeneously dispersed inside the PVA/TA/PAA hydrogel network without breaking the crosslinking structure. In addition, it presents that the mechanical properties can be tuned by the concentration of CNTs. Then, the self-healing behavior was further tested and displayed in **Figure S9** (Supplementary File). The samples were attached for 3 min (180 s), and they showed successfully self-healed to form an integrated structure and could withstand stretching. Compared to without CNT hydrogel, as expected, it showed higher tensile strength while the value of elongation at break decreased. Then, to investigate the potential applicability of PVA/TA/PAA/

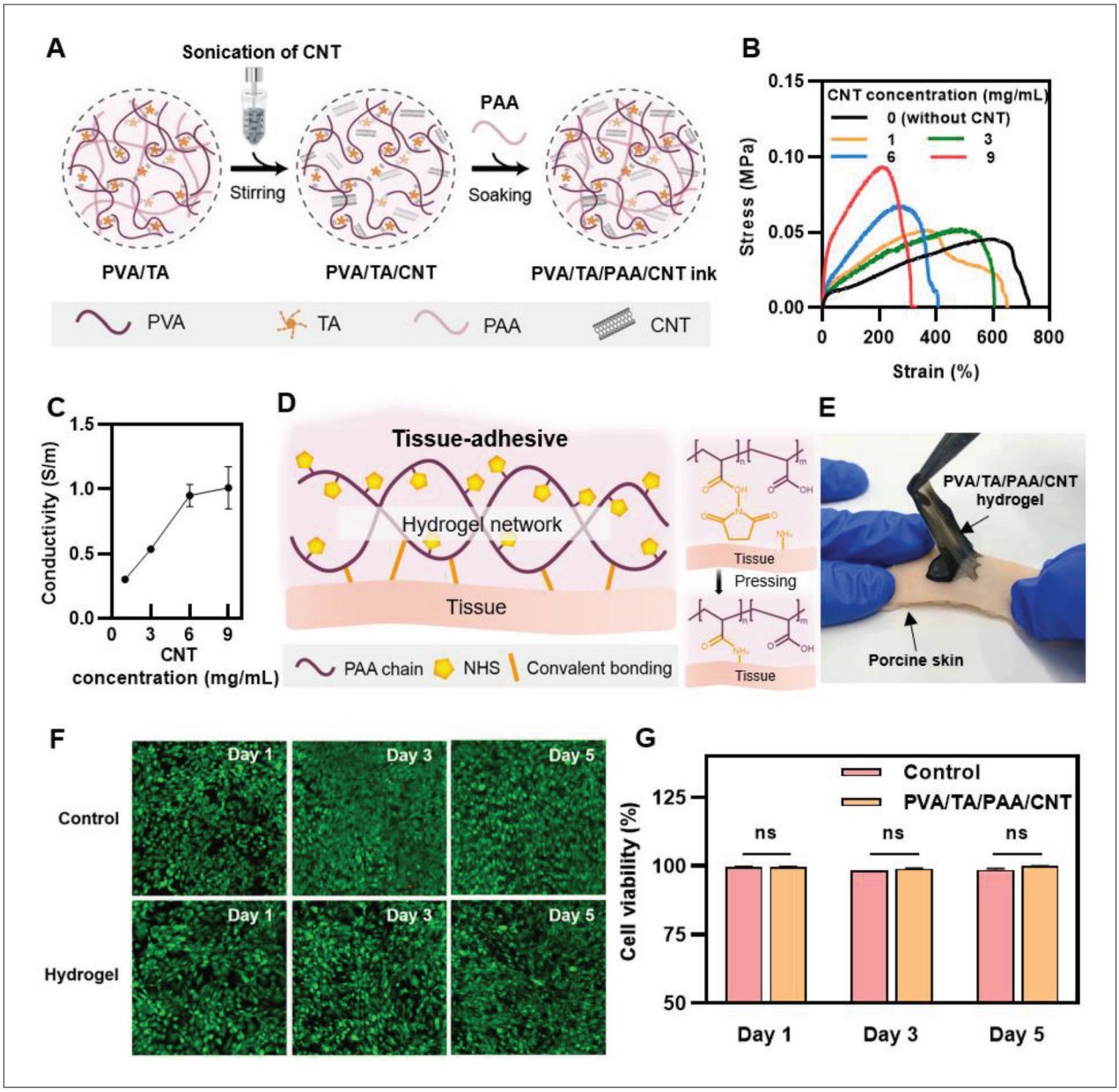

Figure 4. Electrically conductive hydrogel inks. (A) Schematic illustration of the synthesis process of PVA/TA/PAA/CNT hydrogel inks. (B) Stress–strain curves of PVA/TA/PAA/CNT hydrogel with varying CNT concentration. (C) Conductivity as a function of CNT concentration. (D) Schematic illustration of tissue adhesive property of the hydrogel treated with NHS. (E) Photographs of PVA/TA/PAA/CNT hydrogel adhesion on porcine skin. (F) Fluorescent images of *in vitro* biocompatibility test after 1, 3, and 5 days. (G) The percentage of cell viability of *in vitro* biocompatibility test of the hydrogel (ns: no significant differences; $n = 3$; n is the sample size for each group).

CNT hydrogel ink, the conductivity of these hydrogel inks at CNT concentrations of 1, 3, 6, and 9 mg/mL was measured to determine whether the conductivity is sufficient to sense electrophysiological signals from the human body (Figure 4C). The results showed a conductivity of ~0.95 S/m at CNT concentration of 6 mg/mL, which is sufficient, given that the conductivity of human tissue is in the range of 0.3–0.7 S/m[43]. Since the CNT concentration of 6 mg/mL showed the most balanced characteristics, which have high conductivity with good mechanical properties, further experiments were conducted with PVA/$TA_{1:1}$/PAA/CNT hydrogels with the CNT concentration of 6 mg/mL.

3.7. Tissue adhesion and *in vitro* biocompatibility tests

Conformal contact between tissue and electric devices is required for the stable and efficient operation of body signal

transmission. To accurately achieve the human–machine interface, not only flexible, stretchable, and self-healing features but also adhesion capabilities play a very significant role. Recently, Iversen *et al.*[44] presented a flexible, wearable smart patch with Polydimethylsiloxane was defined as PDMS (PDMS) substrate and CNT electrode for pH and hydration sensing. Although they confirmed the pH and hydration sensing ability, they did not feature adhesion functionality which is crucial to wearable sensors. Thus, to enhance the wearability of PVA/TA/PAA/CNT hydrogel, additional surface functionalization via chemical treatment was treated. NHS was introduced on the PAA chain in hydrogel since it has abundant carboxyl groups, which enable the surface having amine groups including tissue to covalently bond[45]. After the contact between the NHS-treated hydrogel and the tissue, the two surfaces are strongly bonded after pressing for 5 min (Figure 4D). As shown in Figure 4E, the PVA/TA/PAA/CNT hydrogel was successfully attached to porcine skin, and also PVA/TA/PAA hydrogel showed strong adhesion (**Figure S10** in Supplementary File).

An *in vitro* biocompatibility test of the hydrogel was also conducted to verify its toxicity for reliable applications to humans. PVA/TA/PAA/CNT hydrogels with NIH 3T3 fibroblasts were incubated in a cell culture media for 5 days, and a live/dead assay was carried out after 1, 3, and 5 days in culture. As shown in Figure 4F, most cells remained alive (green fluorescence) that no obvious cell death was observed on the hydrogel, suggesting excellent biocompatibility. The cell viability tests also showed that no significant differences existed between fibroblasts with the hydrogel and the control group for 5 days (Figure 4G), and as expected, PVA/TA/PAA hydrogel also showed non-toxicity (**Figure S11** in Supplementary File). We confirmed that the proposed hydrogel is biocompatible with tissue and is a safe material for the application.

3.8. Applications of 3D-printed hydrogel: LED lighting test and strain sensing

Figure 5A presents photographs of the circuits printed with PVA/TA/PAA/CNT hydrogel. The printed circuits enable visualization of the proposed hydrogel ink's electrically conductive property through the illumination of an LED. With a printed circuit and power source, the LED bulb was successfully switched on, and when the circuit was physically cut, the LED turned off. However, when the split circuit was put together, the LED turned on instantly through self-healing of the printed hydrogel, and in stretching, the brightness of the light was maintained. Then, as shown in Figure 5B, electrochemical tests were conducted to evaluate the relation between electrical resistance and mechanical deformations. The real-time resistance measurement of the cutting and contacting process revealed that resistance immediately recovered to the initial value after self-healing, which was possible because the reversible network within the hydrogel allows rapid rearrangement of the conductive pathway of the hydrogel. Moreover, conductive hydrogels are suitable for application in resistivity sensors owing to their high sensitivity to mechanical deformation (Figure 5C). As shown in Figure 5D, the relative resistance change ratio upon strain change, $\Delta R(R\text{-}R_0)/R_0 \times 100$ (%), was measured, where the gauge factor (GF) is defined as $(\Delta R/R_0) \times 100/\varepsilon$. It presented a high GF of 1.356 for 0–300% strain and a GF of 4.457 for 300–400% strain, indicating its comparable performance to the previously reported hydrogel-based strain sensor[46,47].

Furthermore, the change in resistance of the printed PVA/TA/PAA/CNT hydrogel ink was evaluated in response to different mechanical inputs, including compression, tension, and stretching. The relative resistance change ratio upon deformation was measured, and the results for compression, tension, and stretching are shown in Figure 5E. The resistance signal was read and recorded by an electrometer, while the printed circuit was in the bending and stretching conditions. As in the earlier experiment, the PVA/TA/PAA/CNT hydrogel sample was printed with dimensions of 100 mm (height) × 200 mm (width) using a 600-μm-diameter nozzle. The compressive, tensile bending, and stretching resistance change ratios reached approximately 30%, 10%, and 100%, respectively. From the electrical performance investigation, we conclude that the hydrogel could be utilized as a strain sensor to accurately detect body movements.

4. Conclusion

In this study, we developed a 3D-printable, tough, self-healing, and electrically conductive hydrogel made from PVA, TA, and PAA. The PVA/TA/PAA hydrogel ink has improved mechanical properties and self-healing capabilities compared to traditional hydrogels due to its double network structure based on reversible hydrogen bonds. TA acts as a crosslinker, forming weak hydrogen bonds on PVA chains, while PAA forms strong hydrogen bonds to create a double network. The PVA/$TA_{1:1}$/PAA ink has impressive toughness, stretchability, and self-healing properties. In addition, the developed hydrogel ink showed excellent printability with a 3D-printing structure and high resolution (~100 μm), compared to existing tough and self-healing hydrogels that are not 3D-printed and have low resolution. Rheological tests were performed to assess the suitability of the hydrogel ink for 3D printing and showed that the PVA/$TA_{1:1}$/PAA ink has ideal properties for precise 2D/3D printing. Additionally, we successfully added CNT fillers to the

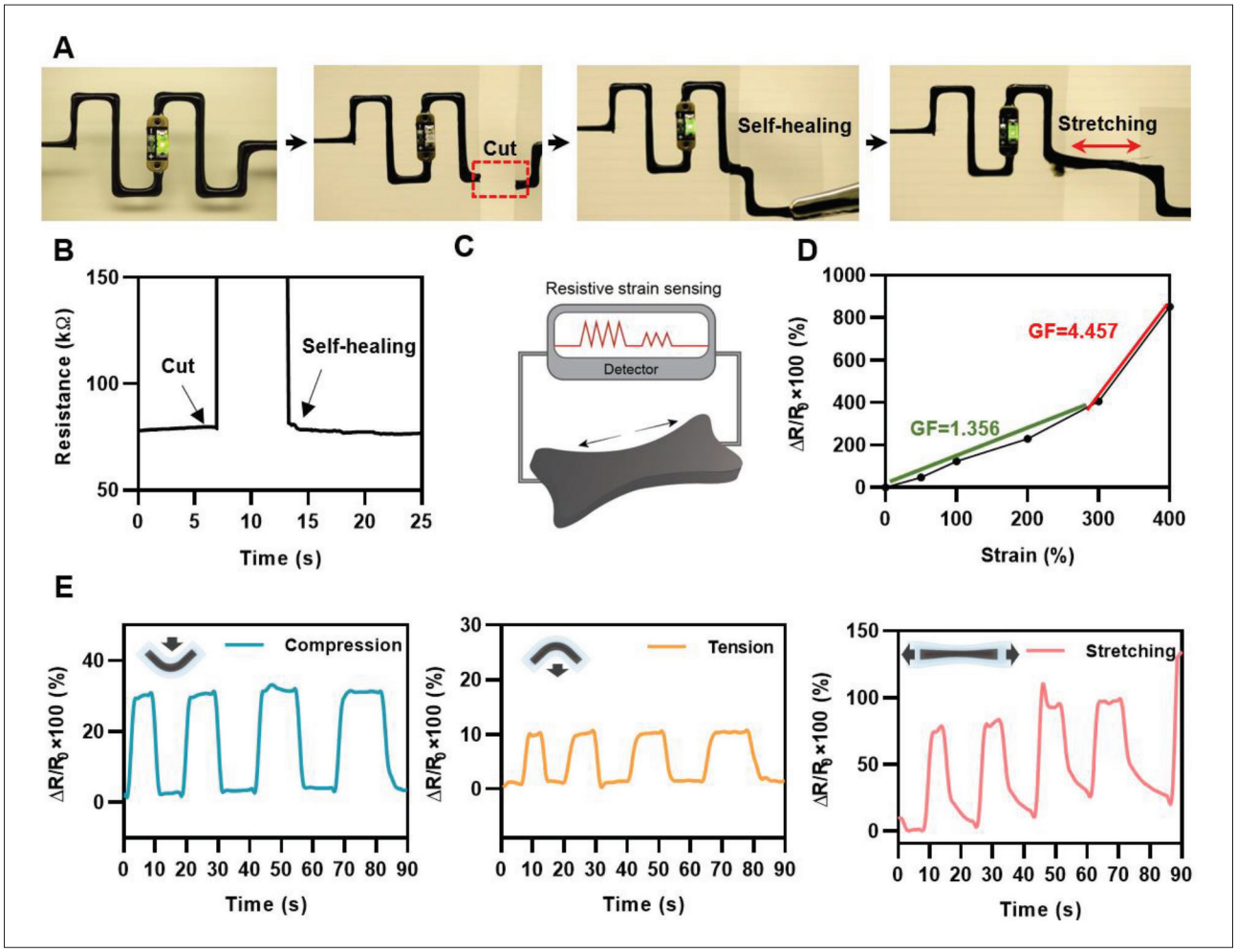

Figure 5. (A) LED lighting tests under self-healing and stretching via the printed circuit with conductive hydrogel inks. (B) Real-time resistance measurement through the cutting and self-healing process of the hydrogel. (C) Schematic illustration of the hydrogel for resistive strain sensing. (D) Relative resistance changes of the hydrogel as a function of applied strain. (E) Strain sensing through resistance change.

PVA/TA/PAA hydrogel ink and confirmed the practicality by demonstrating biocompatibility, tissue adhesiveness, and electrical conductivity with LED lighting and strain sensing tests. This study provides valuable insights for improving the functionality of hydrogel-based inks for practical applications in soft electronics, wearable devices, and smart healthcare systems.

Acknowledgments

None.

Funding

This work was supported by the National Research Foundation of Korea (NRF) funded by Ministry of Science and ICT (Project numbers: 2022M3E5E9082213; NRF 2022R1A2C4001652) and the Yonsei University (RMS2 2022-22-0170).

Conflict of interest

The authors declare no conflict of interest.

Author contributions

Conceptualization: Soo A Kim, Yeontaek Lee, Jae Park, Jungmok Seo
Formal analysis: Soo A Kim, Yeontaek Lee
Methodology: Soo A Kim, Yeontaek Lee, Kijun Park, Jae Park, Soohwan An
Funding acquisition: Jungmok Seo
Investigation: Soo A Kim, Soohwan An, Jinseok Oh, Minkyong Kang, Yurim Lee, Yejin Jo
Project administration: Jungmok Seo, Seung-Woo Cho
Supervision: Jungmok Seo
Writing – original draft: Soo A Kim
Writing – review & editing: Soo A Kim, Kijun Park, Jungmok Seo

Ethics approval and consent to participate

Not applicable.

Consent for publication

Not applicable.

Availability of data

Not applicable.

References

1. Stanford V, 2004, Biosignals offer potential for direct interfaces and health monitoring. *IEEE Pervasive Comput*, 3(1): 99–103.

   https://doi.org/10.1109/MPRV.2004.1269140

2. Swapna M, Viswanadhula UM, Aluvalu R, *et al.*, 2022, Bio-signals in medical applications and challenges using artificial intelligence. *J Sens Actuator Netw*, 11(1): 17.

   https://doi.org/10.3390/jsan11010017

3. Dash A, Cudworth II G, 1998, Therapeutic applications of implantable drug delivery systems. *J Pharmacol Toxicol Methods*, 40: 1–12.

   https://doi.org/10.1002/adma.201902783

4. Liu Y, Yang T, Zhang Y, *et al.*, 2019, Ultrastretchable and wireless bioelectronics based on all-hydrogel microfluidics. *Adv Mat*, 31(39): 1902783.

   https://doi.org/10.1002/adma.201902783

5. Webb RC, Bonifas AP, Behnaz A, *et al.*, 2013, Ultrathin conformal devices for precise and continuous thermal characterization of human skin. *Nat Mater*, 12(10): 938–44.

   http://doi.org/10.1038/nmat3755

6. Gao G, Yang F, Zhou F, *et al.*, 2020, Bioinspired self-healing human–machine interactive touch pad with pressure-sensitive adhesiveness on targeted substrates. *Adv Mat*, 32(50): 2004290.

   https://doi.org/10.1002/adma.202004290

7. Yuk H, Lu B, Zhao X, 2019, Hydrogel bioelectronics. *Chem Soc Rev*, 48(6): 1642–1667.

   http://doi.org/10.1039/C8CS00595H

8. Appel EA, del Barrio J, Loh XJ, *et al.*, 2012, Supramolecular polymeric hydrogels. *Chem Soc Rev*, 41(18): 6195–6214.

   http://doi.org/10.1039/C2CS35264H

9. Kifaro EG, Kim MJ, Jung S, *et al.*, 2022, Direct reverse transcription real-time PCR of viral RNA from saliva samples using hydrogel microparticles. *Biochip J*, 16(4): 409–421.

   http://doi.org/10.1007/s13206-022-00065-0

10. Zhang YS, Khademhosseini A, 2017, Advances in engineering hydrogels. *Science*, 356(6337): eaaf3627.

    http://doi.org/10.1126/science.aaf3627

11. Liu Y, He W, Zhang Z, *et al.*, 2018, Recent developments in tough hydrogels for biomedical applications. *Gels*, 4(2): 46.

    https://doi.org/10.3390/gels4020046

12. Tee BCK, Wang C, Allen R, *et al.*, 2012, An electrically and mechanically self-healing composite with pressure- and flexion-sensitive properties for electronic skin applications. *Nat Nanotechnol*, 7(12): 825–832.

    http://doi.org/10.1038/nnano.2012.192

13. Chen Z, Luo J, Hu Y, *et al.*, 2022, Fabrication of lignin reinforced hybrid hydrogels with antimicrobial and self-adhesion for strain sensors. *Int J Biol Macromol*, 222 (Part A): 487–496.

    https://doi.org/10.1016/j.ijbiomac.2022.09.197

14. Guo Y, Bae J, Fang Z, *et al.*, 2020, Hydrogels and hydrogel-derived materials for energy and water sustainability. *Chem Rev*, 120(15): 7642–7707.

    http://doi.org/10.1021/acs.chemrev.0c00345

15. Lu B, Lin F, Jiang X, *et al.*, 2017, One-pot assembly of microfibrillated cellulose reinforced PVA–borax hydrogels with self-healing and pH-responsive properties. *ACS Sustain Chem Eng*, 5(1): 948–956.

    http://doi.org/10.1021/acssuschemeng.6b02279

16. Billiet T, Vandenhaute M, Schelfhout J, *et al.*, 2012, A review of trends and limitations in hydrogel-rapid prototyping for tissue engineering. *Biomaterials*, 33(26): 6020–6041.

    https://doi.org/10.1016/j.biomaterials.2012.04.050

17. Namgung H, Kaba AM, Oh H, *et al.*, 2022, Quantitative determination of 3D-printing and surface-treatment conditions for direct-printed microfluidic devices. *BioChip J*, 16(1): 82–98.

    http://doi.org/10.1007/s13206-022-00048-1

18. Tan HW, Choong YYC, Kuo CN, *et al.*, 2022, 3D printed electronics: Processes, materials and future trends. *Prog Mater Sci*, 127: 100945.

    https://doi.org/10.1016/j.pmatsci.2022.100945

19. Chen J, Peng Q, Thundat T, *et al.*, 2019, Stretchable, injectable, and self-healing conductive hydrogel enabled by multiple hydrogen bonding toward wearable electronics. *Chem Mater*, 31(12): 4553–4563.

    http://doi.org/10.1021/acs.chemmater.9b01239

20. Jin S, Kim Y, Son D, *et al.*, 2022, Tissue adhesive, conductive, and injectable cellulose hydrogel ink for on-skin direct writing of electronics. *Gels*, 8(6): 336.

21. Wei J, Wang J, Su S, *et al.*, 2015, 3D printing of an extremely tough hydrogel. *RSC Adv*, 5(99): 81324–81329.

    http://doi.org/10.1039/C5RA16362E

22. Song PA, Xu Z, Guo Q, 2013, Bioinspired strategy to reinforce PVA with improved toughness and thermal properties via hydrogen-bond self-assembly. *ACS Macro Lett*, 2(12): 1100–1104.

    http://doi.org/10.1021/mz4005265

23. George J, Sabapathi SN, Siddaramaiah, 2015, Water soluble polymer-based nanocomposites containing cellulose nanocrystals, in *Eco-friendly Polymer Nanocomposites: Processing and Properties*, Thakur VK, Thakur MK (Eds), Springer India, New Delhi, 259–293.

24. Meng Y, Cao J, Chen Y, *et al.*, 2020, 3D printing of a poly(vinyl alcohol)-based nano-composite hydrogel as an artificial cartilage replacement and the improvement mechanism of printing accuracy. *J Mater Chem B*, 8(4): 677–690.

    http://doi.org/10.1039/C9TB02278C

25. Chen W, Li N, Ma Y, *et al.*, 2019, Superstrong and tough hydrogel through physical cross-linking and molecular alignment. *Biomacromolecules*, 20(12): 4476–4484.

    http://doi.org/10.1021/acs.biomac.9b01223

26. Fan H, Wang J, Jin Z, 2018, Tough, swelling-resistant, self-healing, and adhesive dual-cross-linked hydrogels based on polymer–tannic acid multiple hydrogen bonds. *Macromolecules*, 51(5): 1696–1705.

    http://doi.org/10.1021/acs.macromol.7b02653

27. Jafari H, Ghaffari-Bohlouli P, Niknezhad SV, *et al.*, 2022, Tannic acid: A versatile polyphenol for design of biomedical hydrogels. *J Mater Chem B*, 10(31): 5873–5912.

    http://doi.org/10.1039/D2TB01056A

28. Shi S, Peng X, Liu T, *et al.*, 2017, Facile preparation of hydrogen-bonded supramolecular polyvinyl alcohol-glycerol gels with excellent thermoplasticity and mechanical properties. *Polymer*, 111: 168–176.

29. Kang J, Son D, Wang G-JN, *et al.*, 2018, Tough and water-insensitive self-healing elastomer for robust electronic skin. *Adv Mater*, 30(13): 1706846.

    https://doi.org/10.1002/adma.201706846

30. Liu T, Jiao C, Peng X, *et al.*, 2018, Super-strong and tough poly(vinyl alcohol)/poly(acrylic acid) hydrogels reinforced by hydrogen bonding. *J Mater Chem B*, 6(48): 8105–8114.

    http://doi.org/10.1039/C8TB02556H

31. Qin H, Zhang T, Li N, *et al.*, 2019, Anisotropic and self-healing hydrogels with multi-responsive actuating capability. *Nat Commun*, 10(1): 2202.

    http://doi.org/10.1038/s41467-019-10243-8

32. Canadell J, Goossens H, Klumperman B, 2011, Self-healing materials based on disulfide links. *Macromolecules*, 44(8): 2536–2541.

    http://doi.org/10.1021/ma2001492

33. Sun TL, Luo F, Hong W, *et al.*, 2017, Bulk energy dissipation mechanism for the fracture of tough and self-healing hydrogels. *Macromolecules*, 50(7): 2923–2931.

    http://doi.org/10.1021/acs.macromol.7b00162

34. Zhou J, Vijayavenkataraman S, 2021, 3D-printable conductive materials for tissue engineering and biomedical applications. *Bioprinting*, 24: e00166.

    https://doi.org/10.1016/j.bprint.2021.e00166

35. Smith PT, Basu A, Saha A, *et al.*, 2018, Chemical modification and printability of shear-thinning hydrogel inks for direct-write 3D printing. *Polymer*, 152: 42–50.

    https://doi.org/10.1016/j.polymer.2018.01.070

36. Zhou J, Yan H, Wang C, *et al.*, 2022, 3D printing highly stretchable conductors for flexible electronics with low signal hysteresis. *Virtual Phys Prototyp*, 17(1): 19–32.

    http://doi.org/10.1080/17452759.2021.1980283

37. Karolina Pierchala M, Kadumudi FB, Mehrali M, *et al.*, 2021, Soft electronic materials with combinatorial properties generated via mussel-inspired chemistry and halloysite nanotube reinforcement. *ACS Nano*, 15(6): 9531–9549.

    http://doi.org/10.1021/acsnano.0c09204

38. Liu X, Liu J, Lin S, *et al.*, 2020, Hydrogel machines. *Mater Today*, 36: 102–124.

    https://doi.org/10.1016/j.mattod.2019.12.026

39. Lu Y, Biswas MC, Guo Z, *et al.*, 2019, Recent developments in bio-monitoring via advanced polymer nanocomposite-based wearable strain sensors. *Biosens Bioelectron*, 123: 167–177.

    https://doi.org/10.1016/j.bios.2018.08.037

40. Dannert C, Stokke BT, Dias RS, 2019, Nanoparticle-hydrogel composites: From molecular interactions to macroscopic behavior. *Polymers*, 11(2): 275.

    http://doi.org/ 10.3390/polym11020275

41. Sawicki K, Czajka M, Matysiak-Kucharek M, *et al.*, 2019, Toxicity of metallic nanoparticles in the central nervous system. *Nanotechnol Rev*, 8(1): 175–200.

    http://doi.org/doi:10.1515/ntrev-2019-0017

42. Zheng W, Li Y, Xu L, *et al.*, 2020, Highly stretchable, healable, sensitive double-network conductive hydrogel for wearable sensor. *Polymer*, 211: 123095.

    https://doi.org/10.1016/j.polymer.2020.123095

43. Kim T, Park J, Sohn J, *et al.*, 2016, Bioinspired, highly stretchable, and conductive dry adhesives based on 1D–2D hybrid carbon nanocomposites for all-in-one ECG electrodes. *ACS Nano*, 10(4): 4770–4778.

    http://doi.org/10.1021/acsnano.6b01355

44. Iversen M, Monisha M, Agarwala S, 2022, Flexible, wearable and fully-printed smart patch for pH and hydration sensing in wounds. *Int J Bioprint*, 8(1): 447.

http://doi.org/10.18063/ijb.v8i1.447

45. Yuk H, Varela CE, Nabzdyk CS, *et al.*, 2019, Dry double-sided tape for adhesion of wet tissues and devices. *Nature,* 575(7781): 169–174.

http://doi.org/10.1038/s41586-019-1710-5

46. Zhao W, Huang B, Zhu L, *et al.*, 2022, Printable hydrogels based on starch and natural rubber latex with high toughness and self-healing capability. *Int J Biol Macromol*, 218: 580–587.

https://doi.org/10.1016/j.ijbiomac.2022.07.148

47. Park J, Kim JY, Heo JH, *et al.*, 2023, Intrinsically nonswellable multifunctional hydrogel with dynamic nanoconfinement networks for robust tissue-adaptable bioelectronics. *Adv Sci*, 10: 2207237.

https://doi.org/10.1002/advs.202207237